Heterogeneous photochemical aging of soot by NO_2 under simulated sunlight

Chong Han, Yongchun Liu*, Hong He**

Research Center for Eco-Environmental Sciences, Chinese Academy of Sciences, Beijing 100085, China

HIGHLIGHTS

► Sunlight can enhance the photochemical aging process of soot by NO_2.
► Formed nitro compounds can be photolyzed and produce carbonyl species, NO and HONO.
► Combustion conditions can modify photo-reactivity of soot to NO_2.
► Organic carbon provides main active sites to photochemical aging of soot by NO_2.

ABSTRACT

The aging process of soot in the atmosphere can significantly influence its physical and chemical properties. Here, the heterogeneous photochemical aging of soot by NO_2 under simulated sunlight was investigated using *in situ* attenuated total internal reflection infrared spectroscopy. It was observed that simulated sunlight can enhance the aging process of soot by NO_2. The photochemistry of soot with NO_2 led to the formation of various nitro compounds and oxygen-containing species on the soot surface. The photolysis of the surface nitro compounds resulted in various carbonyl groups and gas-phase NO and HONO. The photochemical aging depended on the NO_2 concentrations and combustion conditions of soot production. The soot samples with high content of organic carbon (OC) showed high photochemical reactivity towards NO_2. This means that the active species mainly belong to OC components, which mainly consist of various polycyclic aromatic hydrocarbons (PAHs) and some unidentified components.

© 2012 Elsevier Ltd. All rights reserved.

1. Introduction

Soot aerosols, which are formed during incomplete combustion processes, primarily consist of elemental carbon with a variable fraction of organic materials (Daly and Horn, 2009; Muckenhuber and Grothe, 2006). With an average emission inventory of 8–24 Tg of carbon per year, they are ubiquitous in the atmosphere and account for ~10–15% of the total atmospheric aerosol mass (Khalizov et al., 2010; Penner and Eddleman, 1993). Soot has a direct and indirect impact on the global radiative balance and climate by absorbing solar energy and acting as cloud condensation nuclei (CCN) (Ackerman et al., 2000; Chameides and Bergin, 2002). In addition, soot particles, exhibiting a large specific surface area for heterogeneous interactions, may change the atmospheric composition through chemical reactions of the atmospheric constituents on their surface (Alcala-Jornod and Rossi, 2004; Arens et al., 2001; Bedjanian et al., 2005; Kleffmann and Wiesen, 2005; Lelièvre

et al., 2004; Zhang and Zhang, 2005). Particularly, chemical interactions between soot with NO_x species have attracted considerable attention in the past years since they may play an important role in the NO_x/HNO_3 ratio and in the HO_x balance of the atmosphere (Aubin and Abbatt, 2007; Ammann et al., 1998; Kleffmann et al., 1999; Kalberer et al., 1999; Lelièvre et al., 2004; Munozy and Rossi, 2002; Prince et al., 2002; Stadler and Rossi, 2000).

Once emitted into the atmosphere, soot particles undergo various aging processes through reacting with active species such as HO_2, O_3, NO_2, NO_3, N_2O_5, HNO_3 and H_2SO_4, and photochemical reactions (Bedjanian et al., 2005; Lelièvre et al., 2004; Munozy and Rossi, 2002; Prince et al., 2002; Saathoff et al., 2001; Weitkamp et al., 2007; Zhang and Zhang, 2005). These aging processes can significantly modify the morphology, microstructure, hygroscopicity, and optical properties of soot, thus affecting their environmental effects. Based on reactions between NO_2 and soot in the dark, however, most previous investigations were focused on the NO_2 uptake kinetics and gas phase products such as HONO and NO (Aubin and Abbatt, 2007; Kleffmann et al., 1999; Lelièvre et al., 2004; Stadler and Rossi, 2000). In the dark, soot surfaces are rapidly deactivated under atmospheric conditions because of the depletion of reactive sites (Arens et al., 2001; Aubin and Abbatt, 2007;

* Corresponding author. Tel.: +86 10 62849121; fax: +86 10 62923563.
** Corresponding author. Tel.: +86 10 62849123; fax: +86 10 62923563.
E-mail addresses: ycliu@rcees.ac.cn (Y. Liu), honghe@rcees.ac.cn (H. He).

Khalizov et al., 2010; Lelièvre et al., 2004). Recently, it was found that UV-A radiation can persistently enhance the reaction of NO_2 on organic films or soot (Brigante et al., 2008; Monge et al., 2010), while the mechanism for this promotion effect is still an open question. This indicates that the photoreaction of soot may represent an important route in atmospheric chemistry.

Compared to the uptake of trace gases on soot and formation of gas-phase species, the surface modification of soot due to heterogeneous reaction has not yet been clarified. Only a few papers have investigated changes in the surface composition and microstructure of soot during reaction with NO_2 or O_3 (Akhter et al., 1984; Al-Abadleh and Grassian, 2000; Kirchner et al., 2000; Smith et al., 1988; Smith and Chughtai, 1995; Zelenay et al., 2011). Various nitrogen-containing species such as R–NO_2, R–ONO_2, and R–ONO, have been observed on soot using infrared spectroscopy. Additionally, as for photochemical reaction, only the effects of UV-A radiation on the uptake and formation of gas-phase species have been studied during the reaction of soot with NO_2 (Monge et al., 2010). Thus, the influences of sunlight on the aging of soot have not been clarified yet. In this study, we investigated the changes of surface functional groups on n-hexane soot exposed to NO_2 and simulated sunlight using in situ attenuated total internal reflection infrared (ATR-IR) spectroscopy. The effects of simulated sunlight, combustion conditions of soot production, and NO_2 concentrations were examined in detail. Additionally, the active sites which may belong to organic carbon (OC) or the carbon skeleton in soot are also discussed.

2. Material and methods

Soot particles were obtained by the combustion of n-hexane (AR, Sinopharm Chemical Reagent Lo., Ltd) in a co-flow system. Soot was collected on top of a diffusion flame maintained by an airflow, which was controlled by mass flow meters to regulate the fuel/oxygen ratio. Fuel transport was afforded by a cotton wick extending into the liquid fuel reservoir. The airflow, a mixture of high purity oxygen and nitrogen, had a range of O_2/N_2 ratio from 27.5% to 47.5%. The combustion conditions were expressed as the molar ratio of the consumed fuel to the introduced oxygen (the fuel/oxygen ratio) during combustion process. The fuel/oxygen ratio was in the range of (0.10–0.18). Thus, soot obtained at fuel/oxygen ratios of 0.10 and 0.18 was identified as "fuel-lean soot" and "fuel-rich soot", respectively.

The in situ ATR-IR spectra were recorded using a NEXUS 6700 spectrometer (Thermo Nicolet Instrument Corp.) The fourier transform infrared (FT-IR) spectrometer was equipped with a high-sensitivity mercury–cadmium–telluride (MCT) detector cooled by liquid N_2. Soot particles from the diffusion flame were directly deposited on the ZnSe crystal of the ATR-IR cell, which flitted very fast within the same time (2–3 s) at 4 cm over the flame during soot deposition. Compared to mass of ATR-IR cell, amount of soot deposited on the ZnSe crystal was so small that we cannot measure it due to the limitation of measurement technique. The ATR-IR cell was sealed with quartz glass, through which soot was irradiated by a xenon lamp (500 W) having a continuous emission in the 350–700 nm range and a dominant wavelength at 480 nm. Light of the xenon lamp was transmitted by the optical fiber which was located at 10 cm over the soot samples. Thus, total irradiance of light was 25 mW cm^{-2} at the soot surface. During the irradiation, the ozone concentration was lower than the detection limit (1.5 ppbv) of the ozone monitor (Model 202, 2B Technology). Prior to the reaction of soot with NO_2, the soot was purged by 100 ml min^{-1} N_2 for 1 h at 298 K. Then, NO_2 (160 ppbv–20 ppmv) with high purity N_2 as carrier gas was introduced into the ATR-IR cell, and the total flow rate was 100 ml min^{-1}. The unreacted soot

surface was taken as the reference background spectrum (100 scans, 4 cm^{-1} resolution). In some cases, gas-phase species were also measured using a THERMO 42i chemiluminescence analyzer when NO_2-aged soot was exposed to N_2 and simulated sunlight. The experiments were performed at 298 K under atmospheric pressure.

The effect of organic carbon (OC) on the reactivity of soot was also investigated. Fresh soot was heated to 300 °C in nitrogen to cause loss of OC without modifying the bulk elemental carbon (Daly and Horn, 2009). After being ultrasonically dispersed in H_2O, the heated soot particles were deposited on the ZnSe crystal and purged by 100 ml min^{-1} N_2. When absorption peaks of H_2O were not observed, the samples were exposed to NO_2 transported in a flow of high purity N_2.

Additionally, ultrasonic extraction of fresh soot and reacted soot was performed in the dark using n-hexane. The extracts from fresh soot and soot reacted with NO_2 were also analyzed by GC–MS according to the following parameters: column HP 5MS (internal diameter 0.25 mm, length 30 m, film thickness 0.25 μm), injection volume: 1 μl, inlet temperature: 280 °C, interface temperature: 280 °C K, with the following temperature program: hold for 1 min at 60 °C; increase temperature to 200 °C at 10 °C min^{-1}; hold for 5 min at 200 °C; increase temperature to 220 °C at 5 K min^{-1}; hold for 5 min at 220 °C; increase temperature to 280 °C at 5 K min^{-1}; hold for 10 min at 280 °C.

3. Results and discussion

Fig. 1 illustrates infrared spectra of the "fuel-rich soot" aged by NO_2 for 11 h in the dark and under simulated sunlight irradiation. The unreacted soot surface was taken as the reference background spectrum. The peaks and their assignments are given in Table 1. As shown in Fig. 1A, the infrared spectra exhibited differences in some peaks when soot was exposed to 160 ppbv NO_2 in the dark and under simulated sunlight. To obtain a better IR signal, the subsequent experiments were done at higher concentrations (ppmv) of NO_2. As shown in Fig. 1B, the observed spectrum showed noticeable changes in some bands after soot was exposed to 5 ppmv of NO_2 for 11 h both in the dark and under irradiation. There were great losses of intensity for bands at 3286 and 3040 cm^{-1}, which are assigned to the alkyne C–H and aromatic Ar–H stretch, respectively (Cain et al., 2010; Kirchner et al., 2000). At the same time, a great increase in the intensities of bands at 1553 and 1325 cm^{-1} (R–NO_2) and 1280 cm^{-1} (R–ONO) implies the formation of nitrogen-containing compounds (Akhter et al., 1984; Al-Abadleh and Grassian, 2000; Kirchner et al., 2000). Under simulated sunlight irradiation, the band at 1717 cm^{-1} originates from a non-nitrogen-containing product and is related to ketone carbonyl C=O (Cain et al., 2010). As shown in Fig. 1B, the intensities of Ar–H (3040 cm^{-1}) and C=O (1717 cm^{-1}) under simulated sunlight showed more significant changes than those in the dark. This confirms that sunlight can enhance the heterogeneous aging process of soot by NO_2. Enhanced role of UV/Vis light were also observed during reaction of soot with O_3 by Zelenay et al. (2011) using NEXAFS spectra, in which absorption of aromatic and aliphatic carbon decreased for the combined exposure of soot to O_3 and light.

By comparing infrared spectra in the range of 1650–1000 cm^{-1} which are ascribed to nitrogen-containing species, however, intensities of these bands under the simulated sunlight were less than those in the dark. It seems that sunlight has negative effects on the presence of nitrogen-containing species. The IR spectra of fresh soot remained unchanged when soot was exposed to the simulated sunlight in pure N_2, suggesting that the negative effects are not from photolysis of reactants on fresh soot. In previous study, it was reported that nitroPAHs can photolyze under irradiation (Bejan
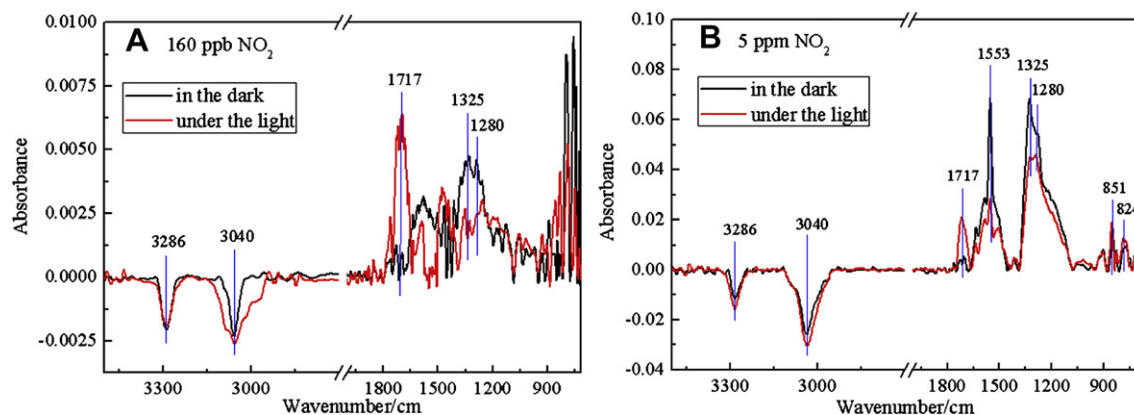
Fig. 1. Comparison of IR spectra of the aged "fuel-rich soot" in 160 ppbv NO_2 (A) or in 5 ppmv NO_2 (B) for 11 h in the dark and under simulated sunlight.

et al., 2006; Feilberg and Nielsen, 2000; Feilberg and Nielsen, 2001; Monge et al., 2010; Sosedova et al., 2011). This indicates that the newly-formed nitro compounds on soot may also photolyze under simulated sunlight, giving rise to the lower intensities of bands in the 1650–1000 cm^{-1} range. To test this assumption, a second set of experiments was performed. Soot samples that had previously been exposed to NO_2 in the dark were then purged by a constant N_2 flow in the dark to promote NO_2 desorption from the surface. When IR spectra stabilized, a reference spectrum was collected and then the light source was turned on. Fig. 2A shows the infrared spectra of the NO_2-reacted soot under simulated sunlight irradiation. A prominent decrease in intensities for R–NO_2 (1560, 1327 cm^{-1}), R–ONO (1275), and R–ONO_2/R–ONO (847, 830 cm^{-1}) indicates the photolysis of nitrogen-containing compounds. Formation of some oxygen-containing groups such as ethers, ketones, aldehydes, lactones and anhydrides, was also determined by the appearance of bands at 1769, 1715, 1690, and 1605 cm^{-1} (Cain et al., 2010; Kirchner et al., 2000).

At the same time, gas-phase products NO_x and NO_y were measured using a chemiluminescence NO_x analyzer when nitrogen-containing compounds on the NO_2-aged soot were irradiated by the simulated sunlight. A denuder tube (10 cm × 1.0 cm i.d.) containing Na_2CO_3 was introduced between the exit of the ATR-IR cell and the detector since HONO is detected as NO_2 by the analyzer. NO and NO_2 together with HONO can be detected using a bypass tube, while only NO and NO_2 can be measured using this denuder because HONO is trapped from the gas stream by Na_2CO_3. Thus, the HONO concentration can be obtained as the difference of the detector signal without and with the carbonate denuder in the sampling line (Monge et al., 2010). The soot aged by NO_2 in the dark was purged by N_2. Once NO and NO_2 were undetectable, the light source was turned on and gas-phase products were measured. Fig. 2B shows the

formation of NO and HONO from the NO_2-aged soot surface under the simulated sunlight. The appearance of HONO has been observed and deduced to be generated from photolysis of the formed nitro compounds when exposed to the UV-A light (Monge et al., 2010; Sosedova et al., 2011). Here, it was definitely observed that the
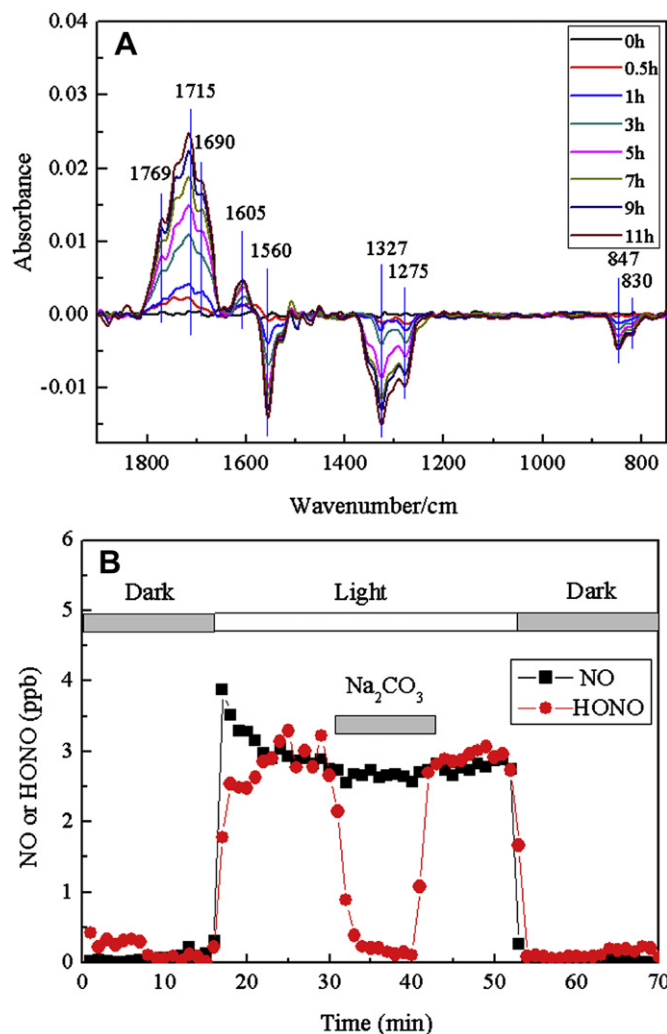

Fig. 2. Photolysis of nitro compounds on the NO_2-reacted soot (A); gas-phase products during photolysis of nitro compounds on the soot aged by NO_2 (5 ppmv) (B).

Table 1
Functional groups observed for fresh and NO_2-aged soot.

Peak/cm^{-1}	Functional group
3286	Alkynes C–H stretch (Kirchner et al., 2000)
3040	Aromatic C–H stretch (Cain et al., 2010)
1717	Carbonyl C=O (Cain et al., 2010)
1553	R–NO_2 asymm stretch (Akhter et al., 1984; Al-Abadleh and Grassian, 2000; Kirchner et al., 2000)
1325	R–NO_2 symm stretch (Akhter et al., 1984; Al-Abadleh and Grassian, 2000; Kirchner et al., 2000)
1280	R–ONO stretch (Akhter et al., 1984; Al-Abadleh and Grassian, 2000; Smith and Chughtai, 1995)
851	R–ONO_2/R–ONO (Al-Abadleh and Grassian, 2000)
824	R–ONO_2/R–ONO (Al-Abadleh and Grassian, 2000)

formed nitro compounds can undergo photolysis under simulated sunlight irradiation. The following possible reaction is accordingly suggested for photo-aging of soot by NO_2:
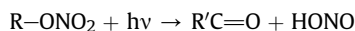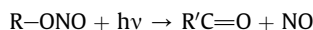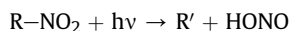
$$R-NO_2 + h\nu \rightarrow R' + HONO$$

$$R-ONO + h\nu \rightarrow R'C=O + NO$$

$$R-ONO_2 + h\nu \rightarrow R'C=O + HONO$$

Fig. 3A exhibits temporal changes of IR spectra in the range of $1660-1440$ cm^{-1} for "fuel-rich soot" during photochemical aging by NO_2. Based on the second derivative spectra (Fig. S1), several overlapping peaks in Fig. 3A were identified and analyzed. Peaks at 1635 and 1590 cm^{-1} are related to R–ONO and R–N–NO_2, respectively (Akhter et al., 1984; Al-Abadleh and Grassian, 2000; Kirchner et al., 2000). Absorption at 1553 cm^{-1} is ascribed to aliphatic R–NO_2 while peaks around 1506 and 1470 cm^{-1} are assigned to aromatic Ar–NO_2 (Akhter et al., 1984; Al-Abadleh and Grassian, 2000; Kirchner et al., 2000). Fig. 3B shows the dynamic changes of the integral areas for bands at 1635, 1590, 1553, 1506 and 1470 cm^{-1}. The curve-fitting results are summarized in Fig. S2. As seen in Fig. 3B, the integrated areas of R–ONO (1635 cm^{-1}), R–N–NO_2 (1590 cm^{-1}), R–NO_2 (1552 cm^{-1}) and Ar–NO_2 (1506, 1470 cm^{-1}) continuously grow as soot is exposed to NO_2 and irradiated by the simulated sunlight. As discussed above, various nitrogen-containing compounds can be formed during the photo-aging process of soot by NO_2.

Fig. S3 shows the evolution of aromatic compounds (Ar–H, $3118-2950$ cm^{-1}), carbonyl compounds (C=O, $1800-1660$ cm^{-1}) and nitrogen-containing compounds (R–N, $1660-1440$ cm^{-1}) on soot during the NO_2 aging process in the dark and under irradiation. As shown in Fig. S3, the exponential patterns suggest that the reactions should be reasonably described by pseudo first-order kinetics. Therefore, the experimental data were fitted using the following pseudo-first-order exponential functions (Ma et al., 2010, 2011; Perraudin et al., 2007),

$$\ln((A_0 - A_p)/(A_t - A_p)) = k_{1,obs}t \qquad (1)$$

where A_t is the peak area at a given time t, A_0 is the initial peak area, and A_p is the peak area of the plateau at 9–11 h in Fig. S3. If the integrated area is directly proportional to the surface concentration, $k_{1,obs}$ is the apparent rate constant of the pseudo-first-order reaction. Fig. 4 displays the linear correlation between peak area
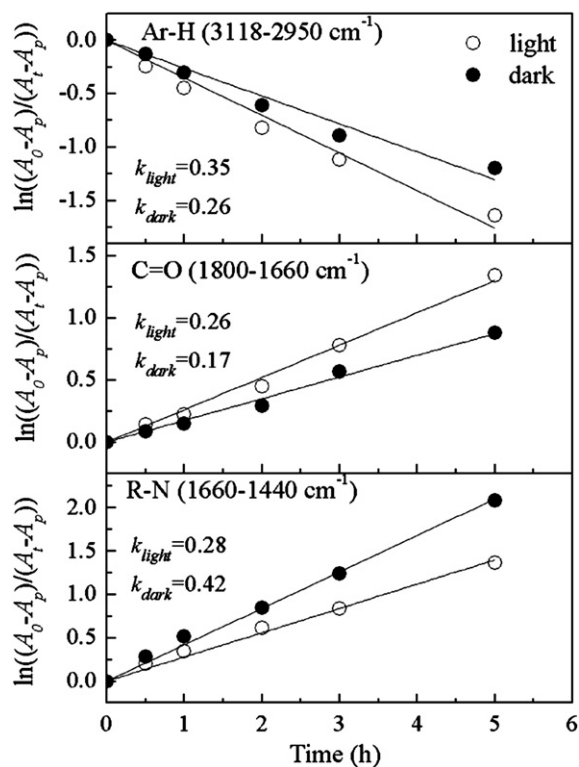

Fig. 4. Kinetics changes of Ar–H (3118–2950 cm^{-1}), C=O (1800–1660 cm^{-1}), and R–N (1660–1440 cm^{-1}) on the "fuel-rich soot" in the dark and under simulated sunlight (5 ppmv NO_2).

changes and irradiation time, exhibiting the first order reaction nature. The $k_{1,obs}$ of the Ar–H, C=O and R–N species was 0.26, 0.17 and 0.42 h^{-1} in the dark, respectively, while the $k_{1,obs}$ of the Ar–H, C=O and R–N species was 0.35, 0.26 and 0.28 h^{-1} under the simulated sunlight, respectively. This demonstrates that $k_{1,obs}$ of Ar–H and C=O species under the simulated light was larger than in the dark, demonstrating that sunlight can enhance the aging of soot by NO_2. The $k_{1,obs}$ of R–N species under the simulated sunlight was less than that in the dark, which can be ascribed to the photolysis of nitro compounds.

In further experiments, soot samples were exposed to different concentrations of NO_2 under the simulated sunlight. Fig. 5 summarizes the kinetic results of the Ar–H, C=O and R–N
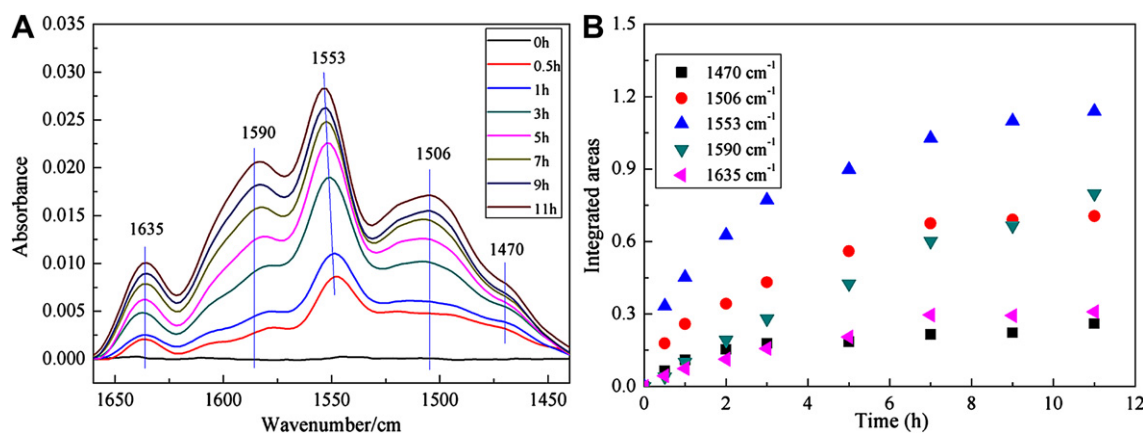

Fig. 3. Temporal changes of *in situ* ATR-IR spectra in the range of 1660–1440 cm^{-1} for "fuel-rich soot" during photo-aging by NO_2 (5 ppmv) (A); Temporal changes in the integrated areas for peaks at 1635, 1590, 1553, 1506, and 1470 cm^{-1} (B).
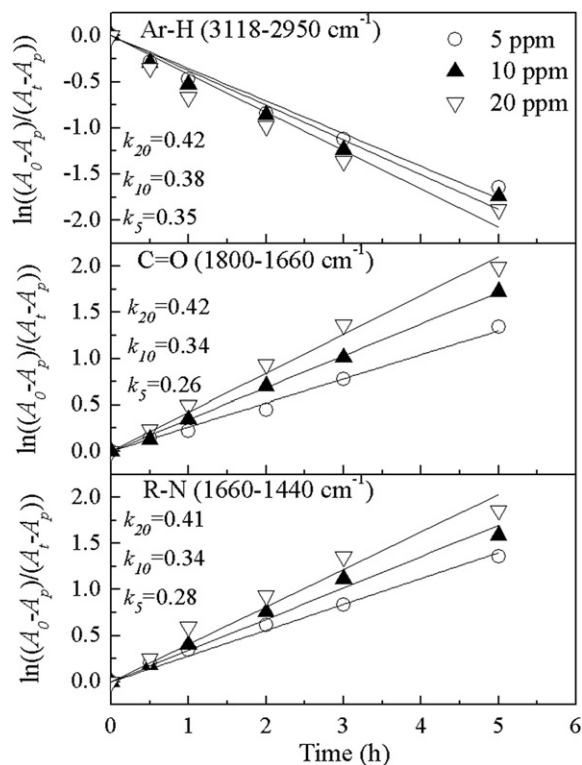
Fig. 5. Kinetics changes of Ar–H (3118–2950 cm^{-1}), C=O (1800–1660 cm^{-1}), and R–N (1660–1440 cm^{-1}) on "fuel-rich soot" in different concentration NO$_2$ under irradiation.

Fig. 6. Kinetics changes of Ar–H (3118–2950 cm^{-1}), C=O (1800–1660 cm^{-1}), and R–N (1660–1440 cm^{-1}) on the "fuel-rich soot" and "fuel-lean soot" (20 ppmv NO$_2$).

species on soot, which show a first-order reaction nature under different NO$_2$ concentrations. As expected, the rates of both R–N and C=O formation and Ar–H loss increased with increasing NO$_2$ concentration. These results indicate that the NO$_2$ concentration can affect the reaction kinetics of surface species on soot under irradiation. It was noticeable that N$_2$O$_4$ can be formed under high NO$_2$ concentrations. According to Akhter et al. (1984) and Sosedova et al. (2011), fast equilibrium between NO$_2$ (g) and NO$_2$ (ads)/N$_2$O$_4$ (ads) should be first built before the reaction with soot and result in a complex mechanism. Additionally, the apparent rate constants of these species under atmospheric conditions should be lower than those in this work because NO$_2$ concentration is only tens of ppbv in the atmosphere.

The same experiment was also performed using "fuel-lean soot" since combustion conditions can significantly modify the surface composition and microstructure of soot. As shown in Fig. 6, the $k_{1,obs}$ of Ar–H, C=O and R–N species for "fuel-lean soot" were less than those for "fuel-rich soot", demonstrating that the fuel/oxygen ratio can significantly affect the reactivity of soot. This coincides with the findings on the effects of combustion conditions on soot reactivity in previous literature (Arens et al., 2001; Chughtai et al., 2002; Monge et al., 2010; Stadler and Rossi, 2000). By comparing IR spectra of the two different types of soot, it was observed that the "fuel-lean soot" showed a stronger peak at 1594 cm^{-1}, related to carbonyl C=O bonded to the aromatic ring (Ar–C=O), and a weaker peak at 3038 cm^{-1} for aromatic Ar–H (Fig. S4). For the "fuel-lean soot", the peak at 3286 cm^{-1} for alkyne C–H disappeared (Fig. S4). Accordingly, the area ratio $A_{Ar-C=O}/A_{Ar-H}$ can be used as an index of the surface oxidation states of soot. In this case, the ratio $A_{Ar-C=O}/A_{Ar-H}$ for "fuel-lean soot" was larger by a factor of 3 than that for "fuel-rich soot". The higher oxygen content in "fuel-lean soot" was also detected using elemental analysis by Stadler and
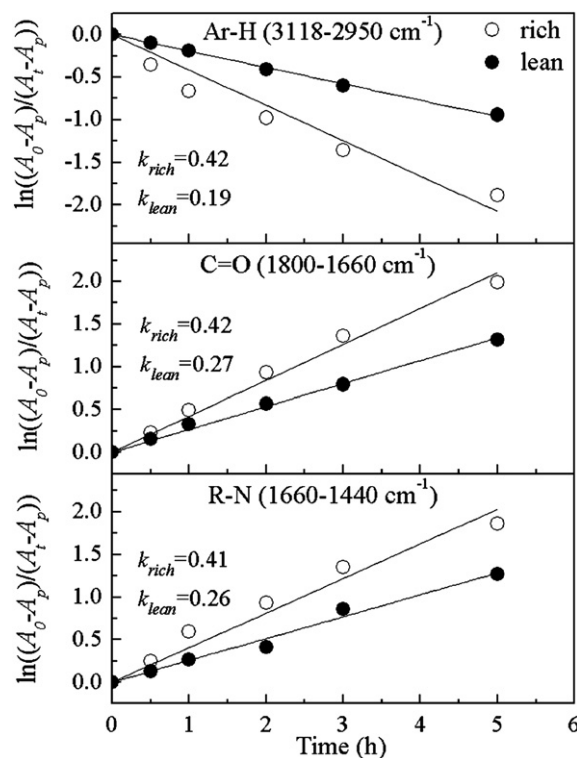
Rossi (2000). This suggests that the "fuel-lean soot" has a higher degree of surface oxidation. During photochemical aging process of soot by NO$_2$, a principal reaction pathway of modification of soot was shown to produce nitrogen-containing compounds and oxygen-related species. Although some oxygen-containing species such as carbonyl compounds may be photosensitizer, a significant increase in the degree of soot surface oxidation greatly diminishes the reduction sites which were main reactants in photochemical reaction. This finally leads to the lower photochemical reactivity of "fuel-lean soot" towards NO$_2$. It should be pointed out that the amount and thickness of the deposited soot may influence diffusion of NO$_2$ into inner layers of soot to modify experimental results. If photochemical aging process of soot by NO$_2$ is the diffusion controlling process, reactivities of soot samples with different compositions should not show a difference under the same reaction conditions. Different groups in one soot sample also exhibit different reactivities to NO$_2$, further determining that photochemical aging process of soot by NO$_2$ is not the diffusion controlling process. Thus, the difference in compositions of different soot samples should be the essence of reason why soot exhibits the reactivities to NO$_2$ under irradiation.

Due to incomplete combustion of hydrocarbon fuels, a broad range of the organic compounds (OC) can be formed, such as saturated and unsaturated hydrocarbons, polycyclic aromatic hydrocarbons (PAHs), and partially oxidized organics (Daly and Horn, 2009; Jonker and Koelmans, 2002; Jonker et al., 2005; Khalizov et al., 2010). The presence of OC condensed on the soot was directly determined by observing a mass decrease (7.0% for "fuel-rich soot" and 3.7% for "fuel-lean soot") through thermal desorption. To investigate roles of OC in the photochemical aging process of soot, "fuel-rich soot" was heated to 300 °C in nitrogen to cause the loss of OC. As shown in Fig. 7, ATR-IR spectra of the heated soot only exhibits the slight changes when samples were exposed to NO$_2$ and
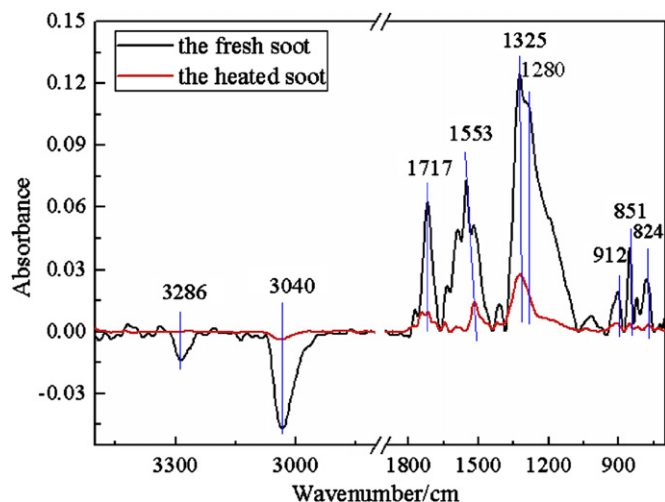
Fig. 7. Comparison of IR spectra of fresh and 300 °C-heated "fuel-rich soot" exposed to NO₂ (20 ppmv) and simulated sunlight for 11 h.

the simulated sunlight for 11 h. It means that the heated soot shows minor photochemical reactivity to NO₂. Therefore, OC should be mainly active sites during the photochemical aging of soot by NO₂.

Based on GC–MS analysis, the composition of the *n*-hexane extracts for fresh and aged soot can be identified. As shown in Fig. 8, the extracts mainly consist of various PAHs (anthracene, phenanthrene, fluoranthene, pyrene, and so on) and some unidentified components. The amount of PAHs with 3–5 rings, such as anthracene, phenanthrene, 4H-lyclopenta[def]phenanthrene, 2-phenylnaphthalene, fluoranthene, pyrene, benzo[ghi]fluoranthene, and cylopenta[cd]pyrene, was decreased after the aging of soot by NO₂. This result demonstrates that PAHs should contribute to the photochemical aging process of soot by NO₂.

In previous papers, it has been found that nitro polycyclic aromatic hydrocarbons (NPAH) can be formed by nitrogen dioxide (NO₂)-initiated oxidation of PAHs in the dark (Chughtai et al., 2002; Gutzwiller et al., 2002; Jonker and Koelmans, 2002; Miet et al., 2009; Smith et al., 1988). Recently, it has been demonstrated that UV-A light can enhance the uptake of NO₂ accompanied with high HONO yields on pyrene, anthracene and polyphenolic solid films (Brigante et al., 2008; George et al., 2005; Sosedova et al., 2011). Monge et al. (2010) also observed persistent reactivity of soot
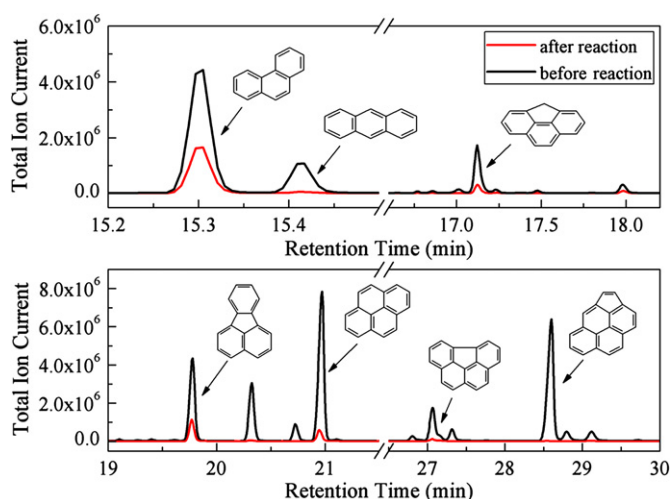

Fig. 8. Total ion chromatogram of the *n*-hexane extracts of fresh "fuel-rich soot" and NO₂-aged soot (20 ppmv, 20 h).

towards NO₂ to produce HONO, NO, and nitrogen-containing organic compounds under UV-A radiation. These results suggested that light can promote the reactivity of PAHs and soot towards NO₂. Besides, formation of HONO or NO has been observed during the photolysis of NPAH and newly-formed nitro compounds under UV-A light (Bejan et al., 2006; Monge et al., 2010; Ammar et al., 2010; Sosedova et al., 2011), suggesting instability of nitro species under irradiation. Due to their extensive π-orbital system, PAHs can absorb sunlight in the visible (400–700 nm) and the ultraviolet regions (290–400 nm) of the solar spectrum (Mallakin et al., 2000). Upon absorbing sunlight, PAHs can be excited to electronically activated states, which can undergo electron or energy transfer followed by nitro compound formation (Monge et al., 2010). As detected during the interaction of soot with NO₂ in this work, simulated sunlight can enhance the reactivity of soot towards NO₂ and cause the photolysis of newly-formed nitro compounds with HONO formation, which can become an atmospheric HONO source. Thus, photochemistry under sunlight may play an important role in the atmospheric chemistry of soot. Photooxidation of PAHs on soot by NO₂ can lead to their degradation or to transformation into NPAH more toxic than the parent compounds (Carrara et al., 2010; Ma et al., 2011). The aging process of soot exposed to NO₂ and the sunlight will be of great importance because this not only influences the fates of PAHs on soot in the atmosphere but also modifies the health impacts of soot. On the other hand, upon exposure to NO₂ and sunlight, nitro compounds and oxygen-containing species formed on soot can become primary adsorption centers of water and increase the hydrophilicity of soot (Zuberi et al., 2005). Therefore, it is strongly suggested that the photochemical aging process of soot by NO₂ can enhance the properties of soot as CCN and ice nuclei (IN). Additionally, a series of environmental effects of soot may be also significantly changed, including the residence of soot in the atmosphere, light scattering and absorption, the greenhouse effect, cloud albedo and precipitation.

4. Conclusions

In this study, enhancement of aging process of soot toward NO₂ by the simulated sunlight was observed. Nitro compounds formed on soot undergone photolysis to produce a series of carbonyl groups and gas-phase NO and HONO. Surface species including Ar–H, C=O, and R–N show a quasi first-order reaction nature during the photochemical aging process of soot by NO₂. Compared to those in the dark, $k_{1,obs}$ of Ar–H and C=O species under the simulated sunlight increased by 35% and 53%, respectively. However, the $k_{1,obs}$ of R–N species under the simulated sunlight was lower than that in the dark due to photolysis under irradiation. Fresh "fuel-rich soot" preheated at 300 °C showed lower reactivity to NO₂, which suggests that organic carbon (OC) mainly contribute to the photochemical aging process of soot by NO₂. Based on GC–MS analysis, polycyclic aromatic hydrocarbons (PAHs) with 3–5 rings and some unidentified components were confirmed to be consumed during the photochemical aging of soot by NO₂.

Appendix A. Supplementary data

Supplementary data related to this article can be found at http://dx.doi.org/10.1016/j.atmosenv.2012.10.008.

References

Ackerman, A.S., Toon, O.B., Stevens, D.E., Heymsfield, A.J., Ramanathan, V., Welton, E.J., 2000. Reduction of tropical cloudiness by soot. Science 288, 1042–1047.

Akhter, M.S., Chughtai, A.R., Smith, D.M., 1984. Reaction of hexane soot with NO_2/N_2O_4. The Journal of Physical Chemistry 88, 5334–5342.

Al-Abadleh, H.A., Grassian, V.H., 2000. Heterogeneous reaction of NO_2 on hexane soot: a Knudsen cell and FT-IR study. The Journal of Physical Chemistry A 104, 11926–11933.

Alcala-Jornod, C., Rossi, M.J., 2004. Chemical kinetics of the interaction of H_2O vapor with soot in the range190 K ≤ T ≤ 300 K: a diffusion tube study. The Journal of Physical Chemistry A 108, 10667–10680.

Ammann, M., Kalberer, M., Jost, D.T., Tobler, L., Rössler, E., Piguet, D., Gäggeler, H.W., Baltensperger, U., 1998. Heterogeneous production of nitrous acid on soot in polluted air masses. Nature 395, 157–160.

Ammar, R., Monge, M.E., George, C., D'Anna, B., 2010. Photoenhanced NO_2 loss on simulated urban grime. ChemPhysChem 11, 3956–3961.

Arens, F., Gutzwiller, L., Baltensperger, U., Gäggeler, H.W., Ammann, M., 2001. Heterogeneous reaction of NO_2 on diesel soot particles. Environmental Science Technology 35, 2191–2199.

Aubin, D.G., Abbatt, J.P.D., 2007. Interaction of NO_2 with hydrocarbon soot: focus on HONO yield, surface modification, and mechanism. The Journal of Physical Chemistry A 111, 6263–6273.

Bedjanian, Y., Lelièvre, S., Bras, G.L., 2005. Experimental study of the interaction of HO_2 radicals with soot surface. Physical Chemistry Chemical Physics 7, 334–341.

Bejan, I., Aal, Y.A.E., Barnes, I., Benter, T., Bohn, B., Wiesen, P., Kleffmann, J., 2006. The photolysis of ortho-nitrophenols: a new gas phase source of HONO. Physical Chemistry Chemical Physics 8, 2028–2035.

Brigante, M., Cazoir, D., D'Anna, B., George, C., Donaldson, D.J., 2008. Photoenhanced uptake of NO_2 by pyrene solid films. The Journal of Physical Chemistry A 112, 9503–9508.

Cain, J.P., Gassman, P.L., Wang, H., Laskin, A., 2010. Micro-FTIR study of soot chemical composition—evidence of aliphatic hydrocarbons on nascent soot surfaces. Physical Chemistry Chemical Physics 12, 5206–5218.

Carrara, M., Wolf, J.-C., Niessner, R., 2010. Nitro-PAH formation studied by interacting artificially PAH-coated soot aerosol with NO_2 in the temperature range of 295–523 K. Atmospheric Environment 44, 3878–3885.

Chameides, W.L., Bergin, M., 2002. Soot takes center stage. Science 297, 2214–2215.

Chughtai, A.R., Kim, J.M., Smith, D.M., 2002. The effect of air/fuel ratio on properties and reactivity of combustion soots. Journal of Atmospheric Chemistry 43, 21–43.

Daly, H.M., Horn, A.B., 2009. Heterogeneous chemistry of toluene, kerosene and diesel soots. Physical Chemistry Chemical Physics 11, 1069–1076.

Feilberg, A., Nielsen, T., 2000. Effect of aerosol chemical composition on the photodegradation of nitro-polycyclic aromatic hydrocarbons. Environmental Science Technology 34, 789–797.

Feilberg, A., Nielsen, T., 2001. Photodegradation of nitro-PAHs in viscous organic media used as models of organic aerosols. Environmental Science Technology 35, 108–113.

George, C., Strekowski, R.S., Kleffmann, J., Stemmler, K., Ammann, M., 2005. Photoenhanced uptake of gaseous NO_2 on solid organic compounds: a photochemical source of HONO. Faraday Discussions 130, 195–210.

Gutzwiller, L., Arens, F., Baltensperger, U., Gäggeler, H.W., Ammann, M., 2002. Significance of semivolatile diesel exhaust organics for secondary HONO formation. Environmental Science Technology 36, 677–682.

Jonker, M.T.O., Hawthorne, S.B., Koelmans, A.A., 2005. Extremely slowly desorbing polycyclic aromatic hydrocarbons from soot and soot-like materials: evidence by supercritical fluid extraction. Environmental Science Technology 39, 7889–7895.

Jonker, M.T.O., Koelmans, A.A., 2002. Sorption of polycyclic aromatic hydrocarbons and polychlorinated biphenyls to soot and soot-like materials in the aqueous environment: mechanistic considerations. Environmental Science Technology 36, 3725–3734.

Kalberer, M., Ammann, M., Gäggeler, H.W., Baltensperger, U., 1999. Adsorption of NO_2 on carbon aerosol particles in the low ppb range. Atmospheric Environment 33, 2815–2822.

Khalizov, A.F., Cruz-Quinones, M., Zhang, R., 2010. Heterogeneous reaction of NO_2 on fresh and coated soot surfaces. Journal of Physical Chemistry A 114, 7516–7524.

Kirchner, U., Scheer, V., Vogt, R., 2000. FTIR spectroscopic investigation of the mechanism and kinetics of the heterogeneous reactions of NO_2 and HNO_3 with soot. The Journal of Physical Chemistry 104, 8908–8915.

Kleffmann, J., Becker, K.H., Lackhoff, M., Wiesen, P., 1999. Heterogeneous conversion of NO_2 on carbonaceous surfaces. Physical Chemistry Chemical Physics 1, 5443–5450.

Kleffmann, J., Wiesen, P., 2005. Heterogeneous conversion of NO_2 and NO on HNO_3 treated soot surfaces: atmospheric implications. Atmospheric Chemistry and Physics 5, 77–83.

Lelièvre, S., Bedjanian, Y., Laverdet, G., Bras, G.L., 2004. Heterogeneous reaction of NO_2 with hydrocarbon flame soot. The Journal of Physical Chemistry A 108, 10807–10817.

Lelièvre, S., Bedjanian, Y., Pouvesle, N., Delfau, J., Vovelle, C., Bras, G.L., 2004. Heterogeneous reaction of ozone with hydrocarbon flame soot. Physical Chemistry Chemical Physics 6, 1181–1191.

Ma, J.Z., Liu, Y.C., He, H., 2010. Degradation kinetics of anthracene by ozone on mineral oxides. Atmospheric Environment 44, 4446–4453.

Ma, J.Z., Liu, Y.C., He, H., 2011. Heterogeneous reactions between NO_2 and anthracene adsorbed on SiO_2 and MgO. Atmospheric Environment 45, 917–924.

Mallakin, A., Dixon, D.G., Greenberg, B.M., 2000. Pathway of anthracene modification under simulated solar radiation. Chemosphere 40, 1435–1441.

Miet, K., Menach, K.L., Flaud, P.-M., Budzinski, H., Villenave, E., 2009. Heterogeneous reactivity of pyrene and 1-nitropyrene with NO_2: kinetics, product yields and mechanism. Atmospheric Environment 43, 837–843.

Monge, M.E., D'Anna, B., Mazri, L., Giroir-Fendler, A., Ammann, M., Donaldson, D.J., George, C., 2010. Light changes the atmospheric reactivity of soot. Proceedings of the National Academy of Sciences of the United States of America 107 (15), 6605–6609.

Muckenhuber, H., Grothe, H., 2006. The heterogeneous reaction between soot and NO_2 at elevated temperature. Carbon 44, 546–559.

Munozy, M.S.S., Rossi, M.J., 2002. Heterogeneous reactions of HNO_3 with flame soot generated under different combustion conditions. Reaction mechanism and kinetics. Physical Chemistry Chemical Physics 4, 5110–5118.

Penner, J.E., Eddleman, H., 1993. Towards the development of a global inventory for black carbon emission. Atmospheric Environment 27A (8), 1277–1295.

Perraudin, E., Budzinski, H., Villenave, E., 2007. Kinetic study of the reactions of ozone with polycyclic aromatic hydrocarbons adsorbed on atmospheric model particles. Journal of Atmospheric Chemistry 56, 57–82.

Prince, P.A., Wade, J.L., Grassian, V.H., Kleiber, P.D., Young, M.A., 2002. Heterogeneous reactions of soot aerosols with nitrogen dioxide and nitric acid: atmospheric chamber and Knudsen cell studies. Atmospheric Environment 36, 5729–5740.

Saathoff, H., Naumann, K.-H., Riemer, N., Kamm, S., Möhler, O., Schurath, U., Vogel, H., Vogel, B., 2001. The loss of NO_2, HNO_3, NO_3/N_2O_5, and HO_2/$HOONO_2$ on soot aerosol: a chamber and modeling study. Geophysical Research Letters 28 (10), 1957–1960.

Smith, D.M., Chughtai, A.R., 1995. The surface structure and reactivity of black carbon. Colloids Surface 105, 47–77.

Smith, D.M., Welch, W.F., Graham, S.M., Chughtai, A.R., Wicke, B.G., Grady, K.A., 1988. Reaction of nitrogen oxides with black carbon: an FT-IR study. Applied Spectroscopy 42, 674–680.

Sosedova, Y., Rouvière, A., Bartels-Rausch, T., Ammann, M., 2011. UVA/Vis-induced nitrous acid formation on polyphenolic films exposed to gaseous NO_2. Photochemical & Photobiological Sciences 10, 1680–1690.

Stadler, D., Rossi, M.J., 2000. The reactivity of NO_2 and HONO on fame soot at ambient temperature: the influence of combustion conditions. Physical Chemistry Chemical Physics 2, 5420–5429.

Weitkamp, E.A., Sage, A.M., Pierce, J.R., Donahue, N.M., Robinson, A.L., 2007. Organic aerosol formation from photochemical oxidation of diesel exhaust in a smog chamber. Environmental Science Technology 41, 6969–6975.

Zelenay, V., Monge, M.E., D'Anna, B., George, C., Styler, S.A., Huthwelker, T., Ammann, M., 2011. Increased steady state uptake of ozone on soot due to UV/Vis radiation. Journal of Geophysical Research 116, D1103.

Zhang, D., Zhang, R., 2005. Laboratory investigation of heterogeneous interaction of sulfuric acid with soot. Environmental Science Technology 39, 5722–5728.

Zuberi, B., Johnson, K.S., Aleks, G.K., Molina, L.T., Molina, M.J., 2005. Hydrophilic properties of aged soot. Geophysical Research Letters 32 (L01807), 1–4.